JB
Journals.ASM.org

The PhoU Protein from *Escherichia coli* Interacts with PhoR, PstB, and Metals To Form a Phosphate-Signaling Complex at the Membrane

Stewart G. Gardner, Kristine D. Johns, Rebecca Tanner, William R. McCleary

Department of Microbiology and Molecular Biology, Brigham Young University, Provo, Utah, USA

Robust growth in many bacteria is dependent upon proper regulation of the adaptive response to phosphate (P_i) limitation. This response enables cells to acquire P_i with high affinity and utilize alternate phosphorous sources. The molecular mechanisms of P_i signal transduction are not completely understood. PhoU, along with the high-affinity, P_i-specific ATP-binding cassette transporter PstSCAB and the two-component proteins PhoR and PhoB, is absolutely required for P_i signaling in *Escherichia coli*. Little is known about the role of PhoU and its function in regulation. We have demonstrated using bacterial two-hybrid analysis and confirmatory coelution experiments that PhoU interacts with PhoR through its PAS (*P*er-*A*RNT-*S*im) domain and that it also interacts with PstB, the cytoplasmic component of the transporter. We have also shown that the soluble form of PhoU is a dimer that binds manganese and magnesium. Alteration of highly conserved residues in PhoU by site-directed mutagenesis shows that these sites play a role in binding metals. Analysis of these *phoU* mutants suggests that metal binding may be important for PhoU membrane interactions. Taken together, these results support the hypothesis that PhoU is involved in the formation of a signaling complex at the cytoplasmic membrane that responds to environmental P_i levels.

Escherichia coli employs seven genes whose products sense environmental phosphate (P_i) and control the expression of the Pho regulon (1, 2). These genes include *phoB*, *phoR*, *pstS*, *pstC*, *pstA*, *pstB*, and *phoU*. Together, these genes are necessary and sufficient for P_i signal transduction. While the identities of the corresponding signaling proteins have been known for some time (3–5), the mechanisms by which they function to transduce the P_i signal have not yet been fully elucidated.

The hub of the signaling pathway consists of the two-component signaling proteins PhoB and PhoR (6). PhoB is a typical winged-helix response regulator that upon aspartyl phosphorylation forms a dimer, which binds to DNA sequences upstream of Pho regulon genes to recruit RNA polymerase and initiate transcription (7–10). PhoR is the bifunctional histidine autokinase/phospho-PhoB phosphatase that donates a phosphoryl group to PhoB when environmental P_i is limiting and removes the phosphoryl group from phosphorylated PhoB (PhoB~P) when environmental P_i is abundant (11, 12). PhoR is an integral membrane protein that does not contain a significant periplasmic domain but does contain a membrane-spanning region (Mem), a cytoplasmic *c*harged *r*egion (CR), a *P*er-*A*RNT-*S*im (PAS) domain (11, 13), with prototypical *D*imerization/*H*istidine *p*hosphorylation (DHp) and *C*atalytic *A*TP binding (CA) domains at its C terminus (14). Since PhoR does not contain a significant periplasmic sensory domain, it is assumed that its PAS domain senses a cytoplasmic signal, but the nature of the signal is not known. Changes in intracellular P_i concentration are not the signal, because these levels remain relatively constant in the presence of various extracellular P_i concentrations and different P_i-signaling states (15, 16).

It has been suggested that the PhoR/PhoB proteins assess P_i availability by monitoring the activity of the Pst transporter (17). The Pst proteins form a type I ATP-binding cassette (ABC) importer that exhibits high-affinity, P_i-specific transport (18–20). PstS is the periplasmic P_i-binding protein, PstC and PstA are integral membrane proteins that form the pore through which P_i passes, and PstB is the dimeric, cytoplasmic ATPase. Based upon data from other well-described ABC transporters (21), P_i-bound PstS likely stimulates the ATPase activity of PstB to facilitate the significant conformational changes that are involved in P_i transport (20). When external P_i levels are above ~4 μM, the transporter exists in a high-activity state that stimulates the phospho-PhoB phosphatase activity of PhoR (5). The low-activity-state transporter signals for the high autokinase activity of PhoR, which leads to elevated levels of phospho-PhoB.

In addition to the four transporter proteins, PhoU is also required for P_i signal transduction but not for transport through the PstSCAB complex (22). When *phoU* is mutated or deleted, PhoR is a constitutive PhoB kinase leading to high expression of the Pho regulon genes. This is accompanied by poor growth and frequently leads to the accumulation of compensatory mutations in *phoR*, *phoB*, or the *pstSCAB* genes. It has been reported that PhoU is a peripheral membrane protein that is a negative regulator of the signaling pathway and that it modulates P_i transport through the PstSCAB proteins (22–24). Multiple crystal structures have been reported for PhoU proteins in various organisms (25–27). Each of the structures shows that PhoU consists of two fairly symmetric, three-alpha-helix bundles (Fig. 1). These structures show several different quaternary structures: monomer, dimer, trimer, and even hexamer. Metal ions are found associated with two of these structures and are coordinated by highly conserved amino acid residues that are found in each three-helix bundle (25, 26). PhoU from *Thermotoga maritima* coordi-

Received 14 January 2014 **Accepted** 15 February 2014
Published ahead of print 21 February 2014
Address correspondence to William R. McCleary, bill_mccleary@byu.edu.
Supplemental material for this article may be found at http://dx.doi.org/10.1128/JB.00029-14.

doi:10.1128/JB.00029-14

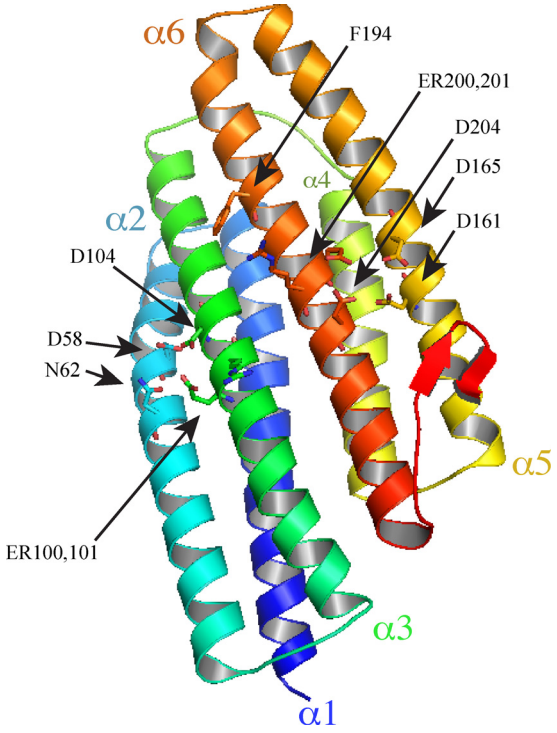

FIG 1 Modeled structure of *E. coli* PhoU. The structure of the PhoU protein from *Escherichia coli* was modeled based upon known structures from the Protein Data Bank using the Phyre2 server. The protein is colored blue to red, going from the amino terminus to the carboxyl terminus. The six helices are labeled from to α1 to α6. The side chains of several highly conserved amino acids are shown. In particular, D58, N62, E100, and D104 form a putative metal binding site between helices 2 and 3, and D161, D165, E200, and D204 form another metal binding site between helices 5 and 6. Also shown is the F194 residue used in the fluorescence assays.

nates trinuclear and tetranuclear iron clusters (25), while PhoU from *Streptococcus pneumoniae* shows zinc ions bound (26). One metal group is bound by residues that correspond to *E. coli* PhoU D58, N62, E100, and D104, and another is bound by D161, D165, E200, and D204 (Fig. 1). It is not known whether these metals are important for physiological function or if they are artifacts of crystallization conditions.

It is not known how PhoU functions in the signaling pathway. However, two general classes of models have been suggested: PhoU may mediate the formation of a signaling complex between the PstSCAB transporter and PhoR (2, 27), or it may produce a soluble messenger that is recognized by the cytoplasmic domains of PhoR (consistent with observations reported by Hoffer and Tommassen [28] and by Rao et al. [29]). No experimental evidence has yet been presented supporting physical interactions between signaling proteins.

We employed bacterial adenylate cyclase two-hybrid (BACTH) analysis as well as coelution experiments to show that PhoU interacts with both PhoR and PstB. Our results show that the PhoU/PhoR interaction involves the PAS domain of PhoR. This is consistent with the presence of a P_i-signaling complex consisting of the PstSCAB transporter, PhoU, and PhoR. We have also shown that the soluble form of *E. coli* PhoU is a dimer that binds manganese and magnesium at conserved sites and that metal binding may be important for localizing PhoU to the membrane.

MATERIALS AND METHODS

Bacterial stains, growth media, and growth conditions. The bacterial strains and plasmids used in this study are shown in Table 1. P1*clr* transductions were carried out as previously described (31). Strains were grown in LB medium (36) at 37°C or in morpholinepropanesulfonic acid (MOPS) defined medium containing either 0.06% glucose and 2.0 mM P_i (MOPS HiP_i) or 0.4% glucose and 0.1 mM Pi (MOPS LoP_i) (37). When indicated, kanamycin, ampicillin, or chloramphenicol was used at 50 μg/ml, 50 μg/ml, or 40 μg/ml, respectively. BACTH strains were grown on MOPS LoP_i plates with 0.2% maltose as a carbon source with ampicillin (50 μg/ml), kanamycin (30 μg/ml), and isopropyl-β-D-thiogalactopyranoside (IPTG) at 0.5 mM and 5-bromo-4-chloro-3-indolyl-β-D-galactopyranoside (X-Gal) at 40 μg/ml. The His-tagged versions of PhoR, PhoU, and PstB and the other site-directed mutants were created using the QuikChange site-directed mutagenesis kit from Agilent Technologies and verified by DNA sequence analysis (see Table S1 in the supplemental material for primer sequences).

***E. coli* PhoU structure prediction.** The three-dimensional structure of the PhoU protein from *E. coli* was predicted by using the Phyre2 web site (http://www.sbg.bio.ic.ac.uk/phyre2) (38). The PhoU sequence was submitted as a query and was analyzed in intensive mode. The server indicated that 216 residues were modeled at >90% accuracy. The predicted structures were displayed using the software program MacPyMol (Schrödinger, LLC).

Bacterial adenylate cyclase two-hybrid analysis. Two-hybrid screens were carried out using the plasmids pKT25 and pUT18C from the BACTH kit and grown in the BTH101 indicator strain (EuroMedex). Control plasmids, coding for T18 and T25 fragments that were fused to a leucine zipper (GCN4), were also provided by the BACTH system kit. Plasmid constructs carrying *phoR*, *phoR* truncations, *pstB*, and *phoU* fusions to the T18 or T25 fragments were generated by cloning PCR fragments that incorporated XbaI and KpnI restriction sites by using the primers listed in Table S1 in the supplemental material. About 1 μl of overnight cultures were spotted on MOPS–maltose–ampicillin–kanamycin–IPTG–X-Gal plates and grown at 30°C until color developed.

β-Galactosidase activity assays. β-Galactosidase has long been utilized as an easily assayable enzyme to measure gene expression, and in the BACTH system, gene expression is linked to protein-protein interactions (31). Assays of β-galactosidase activity were based on methods published previously (39). Specifically, quadruplicate cultures in LB with ampicillin, kanamycin, and IPTG were grown at 30°C with shaking overnight. Then, 50 μl of overnight culture was added to 150 μl LB in a 96-well flat-bottom plate (Greiner Bio-One), and the optical density at 600 nm (OD_{600}) values were read. In addition, in a 1.7-ml centrifuge tube, 200 μl of overnight culture was added to 800 μl of Z buffer (16 g $Na_2HPO_4 \cdot 12H_2O$, 6.25 g $NaH_2PO_4 \cdot H_2O$, 0.75 g KCl, 0.246 g $MgSO_4 \cdot 7H_2O$, and 2.7 ml of β-mercaptoethanol added to 1 liter of water and pH adjusted to 7.0 [39]). One drop of 0.1% SDS and 2 drops of chloroform were added to the cells, and samples were vortexed vigorously for 15 s. The tubes were spun for 1 min at 16,000 × *g* in a benchtop centrifuge to pellet cell debris and chloroform. Two hundred microliters of the cell lysates were then loaded into wells of a 96-well flat-bottom plate. Forty microliters of 0.4% ONPG (*o*-nitrophenyl-β-D-galactopyranoside) in Z buffer was added to each sample, and the OD_{420} values were read once a minute for 30 min in a plate reader that was maintained at 28°C (BioTek Synergy HT). Different units of activity for β-galactosidase activity assays in 96-well plates have been reported for various studies (40, 41). Units of activity were calculated as follows: units = (1,000 × slope of a line fit to OD_{420} in mOD/min)/(4 × OD_{600} of 1:4-diluted overnight sample), based on previously described tests for the BACTH system (39).

PstB/PhoU coelution experiments. Cell cultures were grown overnight in 250 ml MOPS LoP_i medium (except the mixed culture, which combined the Δ*pstB* strain containing pRR48 in 125 ml MOPS HiP_i with the Δ*pstB* strain containing p48pstB-His in 125 ml MOPS LoP_i). Samples were collected by centrifugation at 5,000 × *g* and stored at −20°C. Cell

TABLE 1 Strains and plasmids

Strain or plasmid	Description	Source or reference
E. coli strains		
BW25113	Wild type	30
CSH126	*recA* Tn*10*, Tet^r	31
BM261	P_{pstS}::P_{tac} Δ*pitA*::FRT Δ*pitB*::FRT pRR48	23
BM263	P_{pstS}::P_{tac} Δ*pitA*::FRT Δ*pitB*::FRT Δ*phoU* pRR48	23
BM265	BM263 *pstB*::pBU3 *recA1*, encodes wild-type *phoU*	This study
BM266	BM263 *pstB*::pBQ3 *recA1*, encodes *phoU*Quad	This study
BTH101	F$^-$ *cya-99 araD139 galE15 galK16 rpsL1* (Str^r) *hsdR2 mcrA1 mcrB1*	EuroMedex
BW26337	BW25113 Δ*pstSCAB-phoU*::FRT	30
BW26390	BW25113 Δ*pstB*::FRT	Yale CGSC
JW0390-2	BW25113 Δ*phoR*::*kan*	Yale CGSC
ANCH1	Δ*phoBR*::*kan*	32
SG1	BW26337, Δ*phoBR*::*kan* from ANCH1 by P1*clr* transduction	This study
Plasmids		
pKG116	pACYC184-based replicon, Cam^r, *nahR*	33
p116U2	Cam^r *phoU* expression plasmid, salicylate inducible	23
p116U2His	p116U2 with a C-terminal 6×His tag	This study
p116U2D58A	p116U2 with D58A mutation	This study
p116U2E100A	p116U2 with E100A mutation	This study
p116U2R101A	p116U2 with R101A mutation	This study
p116U2E200A	p116U2 with E200A mutation	This study
p116U2R201A	p116U2 with R201A mutation	This study
p116U2D204A	p116U2 with D204A mutation	This study
p116U2D58A,N62A	p116U2 with D58A and N62A mutations	This study
p116U2E100A,R101A	p116U2 with E100A and R101A mutations	This study
p116U2E200A,R201A	p116U2 with E200A and R201A mutations	This study
p116U2Quad	p116U2 with E100A, R101A, E200A, and R201A mutations	This study
pBU3	Cam^r temp-sensitive, carries *phoU*	This study
pBQ3	Cam^r temp-sensitive, carries *phoU*Quad	This study
pRR48	pBR322-based replicon, Amp^r, *lacI*^{q}	34
pIB307	pMAK705-based vector with a temp-sensitive replicon	35
p48phoR	pRR48-based *phoR* expression plasmid, lactose inducible	This study
p48phoRNHis	p48phoR with an amino-terminal 6×His tag	This study
p48pstB	pRR48 with *pstB* cloned into the NdeI and KpnI sites, lactose inducible	This study
p48pstB-His	p48pstB with a carboxyl-terminal 6×His tag	Ths study
pKT25	Kan^r, BACTH plasmid for T25 fragment of AC	EuroMedex
pUT18C	Amp^r, BACTH plasmid for T18 fragment of AC	EuroMedex
pUT18zip	Amp^r, BACTH plasmid for T18 fragment fused to leucine zipper	EuroMedex
pKT25zip	Kan^r, BACTH plasmid for T25 fragment fused to leucine zipper	EuroMedex
pKT25phoU	Kan^r, BACTH plasmid for *phoU*-T25 fusion	This study
pKT25quad	Kan^r, BACTH plasmid for *phoU*Quad-T25 fusion	This study
pKT25pstB	Kan^r, BACTH plasmid for *pstB*-T25 fusion	This study
pUT18phoU	Amp^r, BACTH plasmid for *phoU*-T18 fusion	This study
pUT18Cquad	Amp^r, BACTH plasmid for *phoU*Quad-T18 fusion	This study
pUT18CD85A	Amp^r, BACTH plasmid for *phoU*D85A-T18 fusion	This study
pUT18CE100A	Amp^r, BACTH plasmid for *phoU*E100A-T18 fusion	This study
pUT18CA147E	Amp^r, BACTH plasmid for *phoU*A147E-T18 fusion	This study
pUT18CE200A	Amp^r, BACTH plasmid for *phoU*E200A-T18 fusion	This study
pUT18CE200A, R201A	Amp^r, BACTH plasmid for *phoU*E200A, R201A-T18 fusion	This study
pUT18CphoRN-C	Amp^r, BACTH plasmid for *phoR*-T18 fusion	This study
pUT18CRN-DHp	Amp^r, BACTH plasmid for N-DHp portion of PhoR-T18 fusion	This study
pUT18CRN-PAS	Amp^r, BACTH plasmid for N-PAS portion of PhoR-T18 fusion	This study
pUT18CRN-CR	Amp^r, BACTH plasmid for N-CR portion of PhoR-T18 fusion	This study
pUT18CRPAS	Amp^r, BACTH plasmid for PhoR PAS-T18 fusion	This study
pUT18CRCR-C	Amp^r, BACTH plasmid for CR-C portion of PhoR-T18 fusion	This study
pUT18CRPAS-C	Amp^r, BACTH plasmid for PAS-C portion of PhoR-T18 fusion	This study
pUT18CRDHp-C	Amp^r, BACTH plasmid for DHp-C portion of PhoR-T18 fusion	This study

pellets were thawed on ice and resuspended in 5 ml PstB lysis buffer (50 mM Tris-HCl [pH 7.2], 300 mM NaCl, and 20 mM imidazole) with protease inhibitor cocktail for use in purification of histidine-tagged proteins (Sigma). Cells were lysed by one passage at 4,000 lb/in^2 and three additional passages at 18,000 lb/in^2 using a Microfluidics LV1 cell disruptor. The crude lysate was then cleared by centrifugation in a Sorval SLA-600 TC rotor at 10,000 × *g* at 4°C for 10 min. An aliquot of the cleared, crude lysate (0.5 ml) was collected and stored at −20°C for later analysis. The remaining cleared crude lysate was loaded onto a fresh 1-ml HisTrap FF nickel column (GE Healthcare). The HisTrap column was then loaded onto a GE Healthcare Akta Prime Plus liquid chromatography system. The column was washed with 20 ml of PstB lysis buffer followed by elution with 5 ml of PstB elution buffer (Tris-HCl [pH 7.2], 300 mM NaCl, and 250 mM imidazole). Wash and elution samples were collected in 1-ml fractions and stored at −20°C before analysis.

PhoR/PhoU coelution experiments. SG1 cells (a Δ*phoB* Δ*phoR* Δ*pstSCAB-phoU* strain) were transformed with p48phoRNHis or pRR48 (as a negative control) and p116U2 (Table 1). Fifty-milliliter cultures were

grown overnight in LB with ampicillin, kanamycin, and 100 μM IPTG. These cells were collected by centrifugation, resuspended in 5 ml PhoU lysis buffer (50 mM Tris, 0.5 M NaCl, 2 mM imidazole, and 14 mM β-mercaptoethanol, pH 7.2) and 25 μl of protease inhibitor cocktail for use in purification of histidine-tagged proteins (Sigma). Then, cells were lysed by one passage at 5,000 lb/in^2 and three passages at 18,000 lb/in^2 through a Microfluidics LV1 microfluidizer. Lysates were cleared by centrifugation, and a lysate sample was taken. Cleared lysates were mixed with 1 ml of nickel-nitrilotriacetic acid (Ni-NTA) agarose slurry (Qiagen) and shaken for 1 h on ice. Samples were then loaded onto a 1-ml disposable polypropylene column (Qiagen); flowthrough was collected and reapplied to the column. Ten milliliters of PhoU lysis buffer was applied for the first wash, followed by 6 ml PhoU wash buffer (like PhoU lysis buffer but with 35 mM imidazole) for the second wash. Finally, 2 ml of PhoU elution buffer (PhoU lysis buffer with 0.5 M imidazole) was applied to elute the bound proteins. We added equal volumes of Laemmli sample buffer (Bio-Rad) to each sample and boiled for 5 min, and 5 μl of each was used for Western blot analysis (the lysate sample was diluted 1:20 to run on the gel).

AP and Western immunoblot assays. The alkaline phosphatase (AP) assays were carried out as described previously (42). The immunoblot assays were performed as described previously (43, 44) using a polyclonal rabbit anti-PhoU antibody and a mouse anti-penta-His antibody (Qiagen). Immunoblots were visualized using the WesternBreeze chemiluminescent Western blot immunodetection kit (Invitrogen).

PhoU purification and gel filtration. The DH5α *E. coli* strain harboring p116U2His was grown overnight in LB medium containing 40 μg/ml chloramphenicol and 100 μM sodium salicylate. Cells were harvested by centrifugation and resuspended in lysis buffer (20 mM $NaPO_4$, 0.5 M NaCl, 20 mM imidazole, 0.5 mM dithiothreitol [DTT], 10% glycerol, and 0.1 mM phenylmethylsulfonyl fluoride [PMSF], pH 7.4), after which they were lysed by one passage at 5,000 lb/in^2 and three passages at 18,000 lb/in^2 through a Microfluidics LV1 microfluidizer. The crude lysate was centrifuged at 12,000 × *g* for 15 min, and the supernatant fraction was used for purification on an Akta Prime-plus chromatography system (GE Healthcare) using a 1-ml HisTrap column as directed by the manufacturer. Specifically, we washed with 20 ml of a mixture of 80% lysis buffer and 10% elution buffer (20 mM $NaPO_4$, 0.5 M NaCl, 0.5 M imidazole, 0.5 mM DTT, and 10% glycerol). Then, we eluted with 100% elution buffer collecting 1-ml fractions. All steps were carried out at a 1-ml/min flow rate. It should be noted that the PhoU-His protein remained soluble only at concentrations below ~0.7 mg/ml, whereas mutant derivatives fell out of solution at concentrations above ~0.1 mg/ml. Gel filtration chromatography was also performed with this system using a HiPrep 16/60 Sephacryl S-200 HR column (GE Healthcare) and a 0.5-ml sample loop run at 0.7 ml/min at 4°C. Standards of 450, 158, 45, 25, and 12.5 kDa were run under the same conditions to create a calibration curve used to predict the size of soluble PhoU.

ICP-MS. Samples of purified PhoU-His were collected from the HisTrap column in 1-ml fractions. For a buffer-only control, the same purification protocol was followed using these same buffers without loading any cell lysate onto the HisTrap column. PhoU-His and the corresponding buffer-only 1-ml fractions were collected during elution and then diluted to 12 ml of 5% nitric acid. These samples were incubated for 3 h at 55°C, centrifuged for 10 min at 2,250 × *g*, filtered through a 0.2-μm Nalgene syringe filter (Thermo Scientific), and analyzed for metal content using inductively coupled plasma mass spectrometry (ICP-MS) on an Elan6000 instrument using the TotalQuant method. We scanned over the whole range using distilled deionized water as the blank and an optimization solution containing 10 ppb of various metals as the standard. Five replicates (each) were performed, and the metal content of the PhoU-His fraction was compared to that of the buffer-only control.

Fluorescence assays for metal binding. To confirm metal binding, we used the PhoU-His F194W protein purified by metal affinity chromatography, dialyzed extensively in dialysis buffer (20 mM sodium phosphate, 0.5 M NaCl, 0.1 mM DTT, and 10% glycerol, pH 7.4), and assayed in a FlouroMax-3 spectrofluorometer with excitation at 280 nm (the excitation wavelength for tryptophan) at 21°C in a temperature-controlled continuously stirred chamber and scanned for fluorescence from 300 to 400 nm. For manganese interactions, we assayed purified protein (70 μg F194W PhoU and 26.4 μg E100A R201A F194W E200A R201A PhoU [QuadW]) in dialysis buffer. To the protein samples, we added 10 mM $MnCl_2$ stepwise to get 5 μM, 25 μM, 75 μM, and 150 μM final concentrations of manganese and scanned the sample for fluorescence. These scans were performed in triplicate. We averaged the fluorescence values for the 345- to 355-nm wavelengths, subtracted the corresponding buffer plus $MnCl_2$ control values, corrected for dilution, and then fit curves to the data to determine the K_d (dissociation constant) and derived the peak fluorescence of each scan. For $MgCl_2$, we followed the same protocol as for $MnCl_2$ but added stocks of $MgCl_2$ stepwise to get 25 μM, 75 μM, 150 μM, 250 μM, 500 μM, 1.5 mM, and 2.75 mM final concentrations.

Integrated strain construction. Temperature-sensitive plasmids carrying a 300-bp fragment of *pstB* upstream of *phoU* were constructed in order to introduce *phoU* (or its mutant derivative) back into the chromosome at its native location. To create the plasmid insert, the 3′ end of the *pstB* gene extending 67 bp into the *phoU* gene was first amplified from chromosomal DNA obtained from BW25113 using the primers PstBfor and PstBrev (see Table S1 in the supplemental material for primer sequences). The *phoU* gene was then amplified from p116U2 or p116U2Quad using the PhoUfor and PhoUrev primers. These two PCR fragments were purified, diluted 1:50, combined, and amplified again using the PstBfor and PhoUrev primers to generate a PCR fragment encoding the 3′ end of the *pstB* gene upstream of *phoU*, exactly as found in the chromosome. This PCR product was subsequently digested with XbaI and HindIII (sites that were engineered into the primers) and ligated into the temperature-sensitive plasmid pIB307, which had been similarly digested. The resulting plasmids were called pBU3 and pBQ3 and carried *phoU* and *phoU* encoding the E100A, R101A, E200A, and R201A substitutions (*phoU*Quad), respectively. The plasmids were then transformed into BM263, which contains a chromosomal deletion of *phoU*, and subsequently grown at 30°C. To select for cells in which the whole plasmid integrated into the chromosome via RecA-mediated recombination in the *pstB* region, several colonies from each transformation were streaked onto fresh LB chloramphenicol plates and incubated at 42°C. To prevent excision of the integrated plasmid, isolated colonies were grown in LB medium at 37°C and then transduced with P1 phage carrying a marked *recA* allele from *E. coli* strain CSH126. The resulting strain with an integrated *phoU* gene was called BM265, and the strain with the integrated quadruple mutant was called BM266. Strains were confirmed by PCR analysis.

Cell fractionation. Membranes were prepared from the indicated strains by harvesting cells from 300 ml of liquid cultures grown to stationary phase in LB. Cells were harvested by centrifugation and resuspended in 14 ml of cold buffer A (phosphate-buffered saline [PBS], 1 mM DTT, and 0.1 mM PMSF, pH 7.2). The cells were then lysed by three to four passages through a Microfluidics M-110L microfluidizer at 4°C. The crude lysates were centrifuged for 10 min at 13,000 × *g* to remove unbroken cells and aggregated proteins, and 5 ml of the supernatant fractions was then subjected to ultracentrifugation at 100,000 × *g* for 1 h at 4°C in an L100XP Beckman Coulter ultracentrifuge using a type 90 Ti rotor. The soluble fractions were saved, and the pelleted fractions were resuspended in 5 ml of 0.1% SDS. Fifty microliters of each fraction was mixed with 50 μl Laemmli sample buffer (Bio-Rad) prepared with β-mercaptoethanol and boiled for 10 min.

RESULTS

Bacterial two-hybrid analysis shows interactions between P_i-signaling proteins. Since preliminary experiments to isolate a stable signaling complex from membranes using affinity chromatography with nonionic detergents were unsuccessful, we employed alternate approaches to address this important question. Since

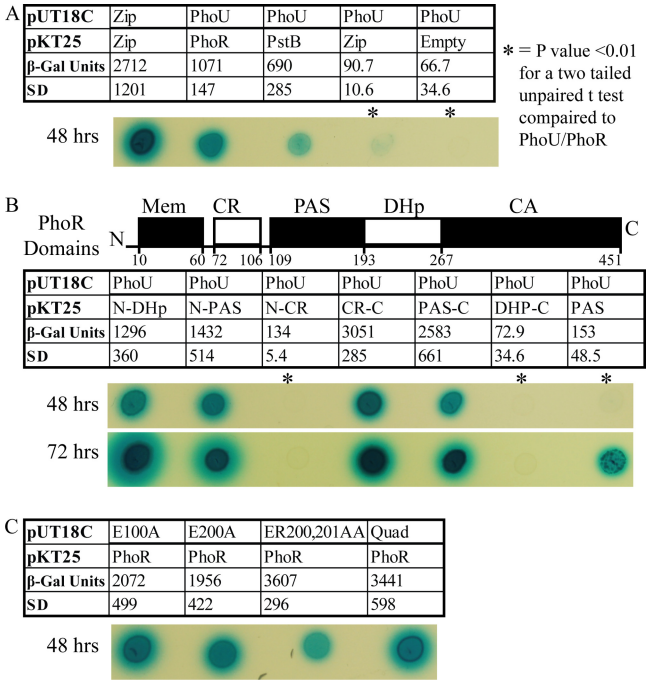

FIG 2 PhoU interacts with PhoR and PstB. A BACTH system was used to investigate interactions of PhoU with other proteins. For a qualitative analysis, cultures were spotted onto MOPS-HiP_i-maltose plates containing X-Gal and incubated at 30°C for the indicated time. All samples shown were from the same plate. For a more quantitative analysis, β-galactosidase assays were performed. The average β-galactosidase activities (β-Gal Units) are reported with the standard deviations (SD) ($n = 4$). (A) PhoU interacts with both PhoR and PstB. Leucine zippers (Zip) fused to the adenylate cyclase domains functioned as a positive control, whereas PhoU paired with the Zip plasmid or an empty vector functioned as negative controls. (B) PhoU interactions with nested deletions of PhoR. Constructs without the PAS domain have significantly fewer interactions than full-length PhoR. The PAS domain alone shows weak interactions with PhoU as observed with color development after 72 h, as well as significantly higher β-galactosidase units than either of the negative controls (two-tailed *t* test gave *P* values of <0.05). (C) PhoU mutants interact with PhoR.

PhoU, PstB, and PhoR are predicted to be found at the cytoplasmic surface of the cytoplasmic membrane, we probed for interactions between these proteins. We conducted bacterial two-hybrid experiments using the BACTH system. When the T18 and T25 domains of adenylate cyclase from *Bordetella pertussis* are in close proximity, they create an active enzyme that produces cyclic AMP (cAMP). By attaching proteins to the T18 and T25 fragments, cAMP production is a measure of whether the fused proteins interact. Since cAMP binds to cAMP receptor protein (CRP), cAMP can be measured indirectly by assaying certain catabolic gene products, such as β-galactosidase. We prepared plasmids that expressed T18-PhoU, T25-PhoR, and T25-PstB and introduced various combinations into an *E. coli* strain that was deleted for adenylate cyclase (BTH101). The strains were plated on MOPS-maltose plates containing X-Gal to provide a qualitative measure of β-galactosidase activity. For a more quantitative evaluation of protein interactions, we performed β-galactosidase assays in 96-well plates. We found that PhoU interacted with both PhoR and PstB, with the PhoU/PhoR interaction being stronger than that for PhoU/PstB (Fig. 2A). We did not observe interactions between T18-PhoU and the T25 domain alone or the T25 domain fused to a leucine zipper. Interactions between T25-PhoU and T18-PhoR and T18-PstB were also detected (data not shown).

Several nested deletions of *phoR* were constructed to identify the region(s) of the protein that interacts with PhoU (Fig. 2B). The deletions were named PhoRN-(domain name) to indicate a protein that extends from the amino terminus of PhoR through a particular domain or PhoR(domain name)-C when deletions removed residues from the amino terminus. The PhoRN-DHp and PhoRN-PAS constructs showed that the CA and DHp domains were not required for the PhoU interaction. Importantly, the interaction was lost when the PAS domain was removed (PhoRN-CR). When PhoR was truncated from the amino terminus, we found that neither the membrane-spanning region nor the CR was required for interaction (PhoRCR-C and PhoRPAS-C), but loss of the PAS domain again disrupted the interaction (PhoRDHp-C). The PAS domain alone showed a weak interaction with PhoU. PhoU fused with T25 and PhoR truncations with T18 gave similar results (data not shown).

PstB and PhoR coelute with PhoU during affinity chromatography. As a complementary method, we employed protein coelution experiments using His-tagged versions of either PstB or PhoR. The *pstB* gene was cloned into pRR48 to express versions of PstB with and without a C-terminal 6×His tag, and both constructs were tested for signaling. P_i signaling is apparent under P_i-replete conditions because cells produce small amounts of alkaline phosphatase (AP). In contrast, elevated AP levels are observed when signaling is defective, such as when mutations occur in any of the *pstSCAB* genes, *phoU*, or even *phoR*. Wild-type cells also display high AP levels when grown in low-P_i medium.

Under high-P_i growth conditions, Δ*pstB* strains expressing either *pstB* or *pstB*-His exhibited low AP levels, indicating that a functional signaling pathway was reconstituted (see Fig. 3A). The empty-vector strain showed elevated AP levels. However, under low-P_i conditions, while the p48*pstB* strain demonstrated an expected increase in AP activity, the strain carrying p48*pstB*-His exhibited low AP levels. This indicates that the *pstB*-His construct constitutively signaled a high-P_i environment regardless of the P_i levels in the growth medium.

We were aware that potential interactions between PstB and PhoU could be transient and difficult to detect due to the large conformational changes that occur in the PstSCAB protein as a consequence of P_i transport. We also recognized that the PstB-His construct may have the fortuitous effect of trapping a complex between PstB and PhoU because it is locked into a "high-P_i" signaling conformation, making the PstB/PhoU interaction easier to detect.

We next tested whether interactions between PstB and PhoU occurred by retaining PstB-His on a HisTrap nickel column along with any interacting proteins and then performing immunoblotting with the subsequent lysate and elution fractions. Since we required elevated expression levels of the Pst transporter and the strains expressing PstB-His were repressed for the Pho regulon, we chose to mix extracts from two Δ*pstB* strains to detect protein-protein interactions. The first strain harbored the pRR48 plasmid and highly expressed the *pstSCA-phoU* operon (including *phoU*) but was missing PstB. The second strain harbored p48*pstB*-His and expressed elevated levels of PstB-His but did not produce the other Pst proteins or PhoU. Cells were grown in MOPS HiP_i medium, pelleted, and mixed together before disruption. The cleared, lysed sample was incubated for several minutes on ice,

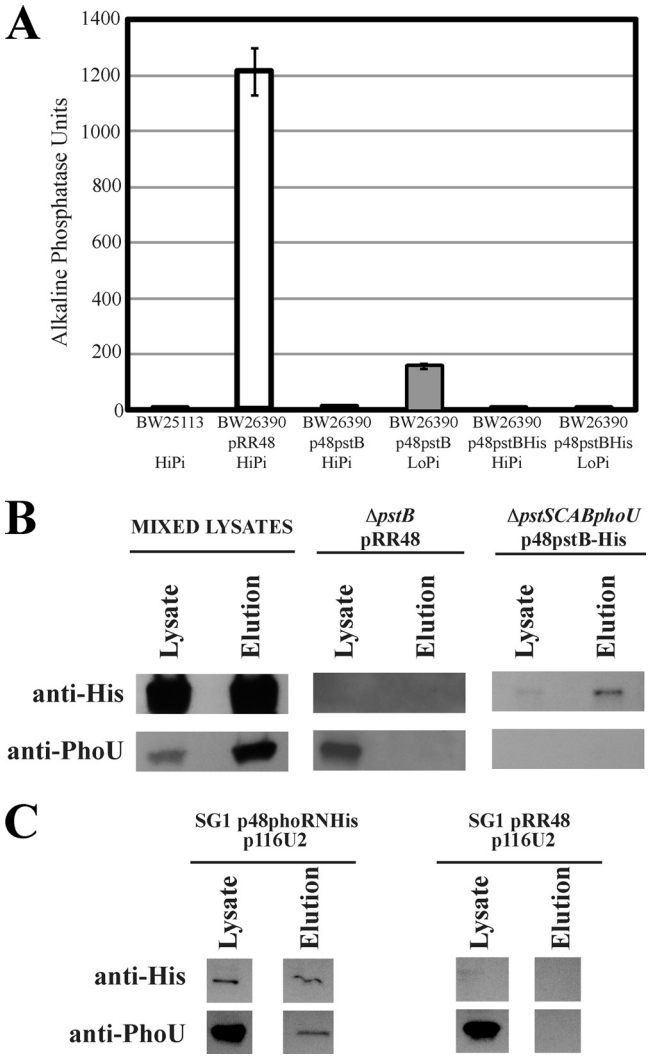

FIG 3 PstB and PhoR coelute with PhoU. (A) Genetic complementation of a Δ*pstB* mutation with p48*pstB* and p48*pstB*-His. The Δ*pstB E. coli* strain BW26390 was transformed with the indicated plasmids, and AP assays were performed. Cells were grown in MOPS HiP$_i$ or MOPS LoP$_i$ medium, where indicated. (B) Binding of PhoU to PstB-His. Cells were lysed, and the soluble extracts were subjected to nickel affinity purification by passage over a HisTrap column. Identical samples from the lysate and elution fraction were separated by SDS-PAGE, transferred to nitrocellulose membranes, and analyzed by immunodetection. The mixed lysate sample contained extracts from a strain expressing high levels of PstS, PstC, PstA, and PhoU with a sample expressing high levels of PstB-His. The use of the mixed lysate was necessary because the expression of PstB-His decreased the expression of the Pho regulon in the Δ*pstB* genetic background. (C) Plasmids expressing PhoR-His (PhoR with an amino-terminal 6×His tag) and PhoU were both transformed into a Δ*phoBR* Δ*pstSCAB-phoU* strain (SG1). Nickel affinity chromatography was used to retain the PhoR-His on the affinity column. Cell lysate and elusion fractions were analyzed by Western blotting to see that PhoU coelutes with PhoR-His.

subjected to affinity chromatography, and then processed for Western immunoblotting with anti-His antibody to detect the PstB-His protein and with anti-PhoU antibody to detect PhoU. The mixed sample showed bands for PstB-His and PhoU in the lysate and elution fractions (Fig. 3B). These results demonstrated that PstB-His retained PhoU on the column through the washing procedure. A Δ*pstB* strain harboring the empty vector pRR48 was grown in MOPS LoP$_i$ medium and subjected to the same protocol. As shown in Fig. 3A, this strain constitutively expressed high levels of AP and also produced elevated amounts of PhoU (Fig. 3B, central panel). No PstB-His was observed in any fraction, but a strong PhoU band was observed only in the crude fraction, indicating that PhoU does not bind to the HisTrap nickel column in the absence of PstB-His. When a Δ*pstSCAB-phoU* strain containing p48*pstB*-His was analyzed, it showed low-level expression of PstB-His in the crude fraction but accumulation in the elution fraction. This strain also showed the absence of PhoU in every fraction, indicating that the antibody was specific for PhoU.

We also confirmed the PhoU/PhoR interaction with coelution experiments. We constructed a plasmid that expressed PhoR with an amino-terminal 6×His tag (p48PhoRNHis) and confirmed its signaling activity by introducing it into the Δ*phoR* deletion strain JW0390-2 (45) and performing AP assays (data not shown). Because of difficulties with protein expression levels in this genetic background, we assayed interactions between PhoR and PhoU in SG1, a strain in which genes for all seven of the P$_i$-signaling proteins were deleted. Either pRR48 or p48PhoRNHis was introduced into the SG1 strain containing p116U2. The new strains were grown in LB medium, pelleted, lysed, and subjected to affinity chromatography. Figure 3C shows that PhoU was observed in the lysate fractions of both strains but was found in the elution fraction only when PhoR-His was also present. The anti-His antibodies showed that PhoR-His was produced only when SG1 harbored p48PhoRNHis. These results show that PhoU interacts with both PhoR and PstB, and they are consistent with the presence of a P$_i$-signaling complex. To further understand the role of PhoU in P$_i$ signaling, we characterized its native structure, explored the functions of the its most highly conserved residues by mutational analysis, and determined whether PhoU binds metal ions.

***E. coli* PhoU forms a dimer.** We cloned *phoU*, to encode a native protein or a version with a C-terminal 6×His tag (PhoU-His), into pKG116 and confirmed that the constructs were functional by complementation analysis (data not shown). We then purified PhoU-His using immobilized metal ion affinity chromatography and analyzed its native structure using gel filtration chromatography. Under nonreducing conditions, PhoU-His (with a predicted molecular mass of 28,240 Da) eluted in several peaks corresponding to high-molecular-mass oligomers (data not shown). The oligomers were resolved when β-mercaptoethanol was included in the sample buffer. We think that these oligomers represent nonfunctional forms of PhoU because the side chains of each of its five Cys residues are predicted to extend toward the interior of the protein. Any covalent bonds involving these Cys residues would require PhoU to be partially or completely unfolded. When PhoU-His was analyzed with β-mercaptoethanol in the column buffer, it eluted as a single peak with an apparent molecular mass of 52.1 kDa, which is comparable to the predicted molecular mass of a PhoU dimer (Fig. 4A).

We used the BACTH system to confirm our gel filtration experiments. Using compatible plasmids that expressed T18-PhoU and T25-PhoU, we observed that PhoU interacts with itself (Fig. 4B). We did not observe interactions when T18-PhoU was coexpressed with the T25 fragment alone or when T25-PhoU was coexpressed with the T18 fragment.

***E. coli* PhoU binds manganese and magnesium.** To screen for metals bound to PhoU, the PhoU-His protein was purified and analyzed by inductively coupled plasma mass spectrometry (ICP-MS). We identified manganese as a potential bound metal because

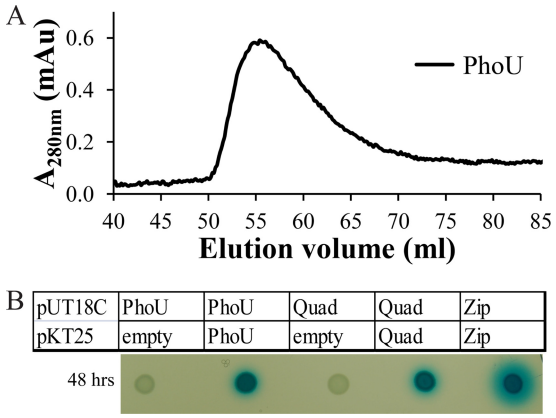

FIG 4 PhoU forms a dimer. (A) *E. coli* PhoU-His was purified and analyzed on a gel filtration column. The PhoU-His protein eluted as a single peak at an elution volume between previously run 45-kDa and 68-kDa standards. PhoU-His has a predicted molecular mass of 28.2 kDa, so this peak corresponds with the expected size of a PhoU dimer. (B) BACTH analysis of PhoU interactions with itself. Strains grown in LB medium with different combinations of plasmids were spotted onto MOPS-HiP_i-maltose plates containing X-Gal and incubated at 30°C.

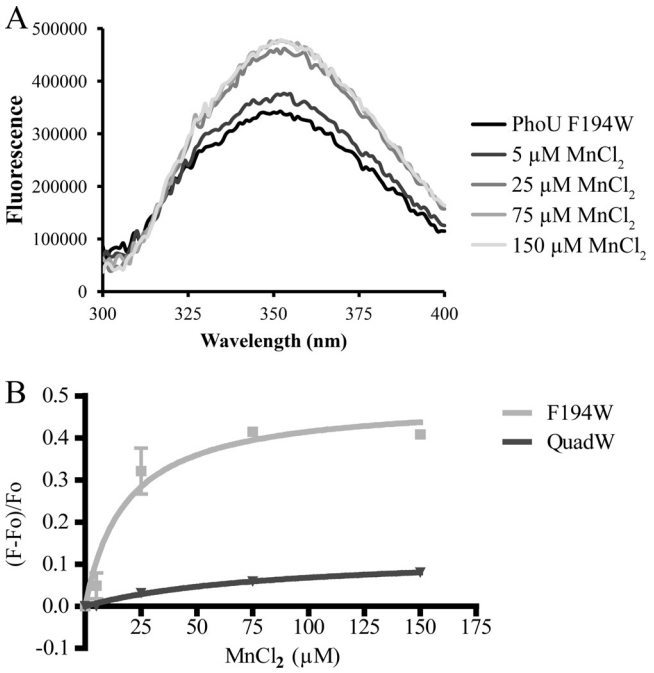

FIG 5 PhoU binds manganese. (A) A representative emission scan of tryptophan fluorescence when purified *E. coli* PhoU-His F194W (F194) was mixed with increasing levels of manganese and excited at 280 nm. The addition of manganese caused an enhancement of the fluorescence and a shift in the peak fluorescence. (B) Manganese binding curve. With the addition of manganese, the mean change in fluorescence between 345 nm and 355 nm was plotted, and a binding curve was fit to the data (error bars represent ± standard errors; $n = 3$).

significantly more manganese was found with the PhoU-His sample than with a buffer only control (*t* test with a *P* value of 2.4×10^{-7}). Nickel and zinc were also identified as potentially binding to PhoU; however these metals may be artifacts from the 6×His tag. We did not detect a significant increase in iron in the sample containing PhoU compared with the control.

We then used a fluorescence assay to further investigate metal binding by PhoU. Tryptophan fluorescence intensity changes and the maximum wavelength shifts when the polarity of its local environment changes. Assays that follow changes in intrinsic tryptophan fluorescence are frequently used to detect changes in local protein environments (46). We engineered a PhoU-His F194W mutant and confirmed that the construct is still functioned in P_i signaling (data not shown). This engineered tryptophan is located 6 residues upstream of the conserved putative metal binding residue, E200, and is on the same face of the α-helix as one of the predicted metal binding sites (Fig. 1). PhoU-His F194W was excited at 280 nm, and emission was followed from 300 to 400 nm. When manganese was added to the sample, fluorescence was enhanced in a pattern that fit a predicted binding curve (Fig. 5A). Fitting a curve to the peak fluorescence values with various concentrations of manganese, we found that PhoU-His F194W bound manganese with an apparent K_d (dissociation constant) of 18.3 μM, with a standard error of 6.2, based on three replicates (Fig. 5B). This value is similar to intracellular levels of manganese in *E. coli* reported between 15 μM (47) and 21.1 μM (48), although it is proposed that the free manganese levels in *E. coli* are much lower than this (49). Magnesium and manganese often overlap in function for cellular processes, and magnesium is at much higher concentrations in the cell than manganese (50). So, we also tested whether the PhoU-His F194W protein bound magnesium and found that it bound this metal with a K_d of ~1.5 ± 0.68 mM (see Fig. S3 in the supplemental material). The high K_d for magnesium may explain why we did not observe this metal bound to PhoU in the ICP-MS experiment. Since the amount of free magnesium in *E. coli* cell is between 1 and 2 mM (51), binding this metal may be important for its physiological function. We saw a shift in the wavelength of peak fluorescence with metal binding. We did not see any significant fluorescence change with zinc or nickel (data not shown). Zinc and nickel are known to bind to 6×His tags (52). Apparently, binding at the C-terminal 6×His tag is far enough away that it does not alter F194W construct fluorescence.

Mutational analysis of conserved residues. To examine the role of metal binding in P_i signaling, we mutated the *phoU* gene to encode proteins in which several of the highly conserved charged residues were converted to alanine residues. These plasmids were introduced into a Δ*phoU* strain in which the *pstSCAB-phoU* promoter was replaced with a lactose-inducible promoter (BM263) to prevent the poor-growth phenotype seen in *phoU* mutants that overexpress a functional PstSCAB transporter (23). Strains were grown overnight in a high-P_i medium, and AP assays were performed to assess signaling (Fig. 6A). Each of the mutants displayed nearly wild-type signaling activity, repressing the expression of alkaline phosphatase. The strongest phenotype was associated with the R201A mutation, which still left PhoU with nearly 80% of its wild-type activity. Immunoblot analysis showed that each of the mutant proteins was expressed at a level similar to those of the others (data not shown).

We created three mutants that carried two mutations in a single site, D58A/N62A, E100A/R101A, and E200A/R201A, to test if it was necessary to alter more than a single residue within a putative metal binding pocket to block function. Each of these double mutants also retained significant PhoU signaling activity. We then created a quadruple mutant which had mutations in each three-

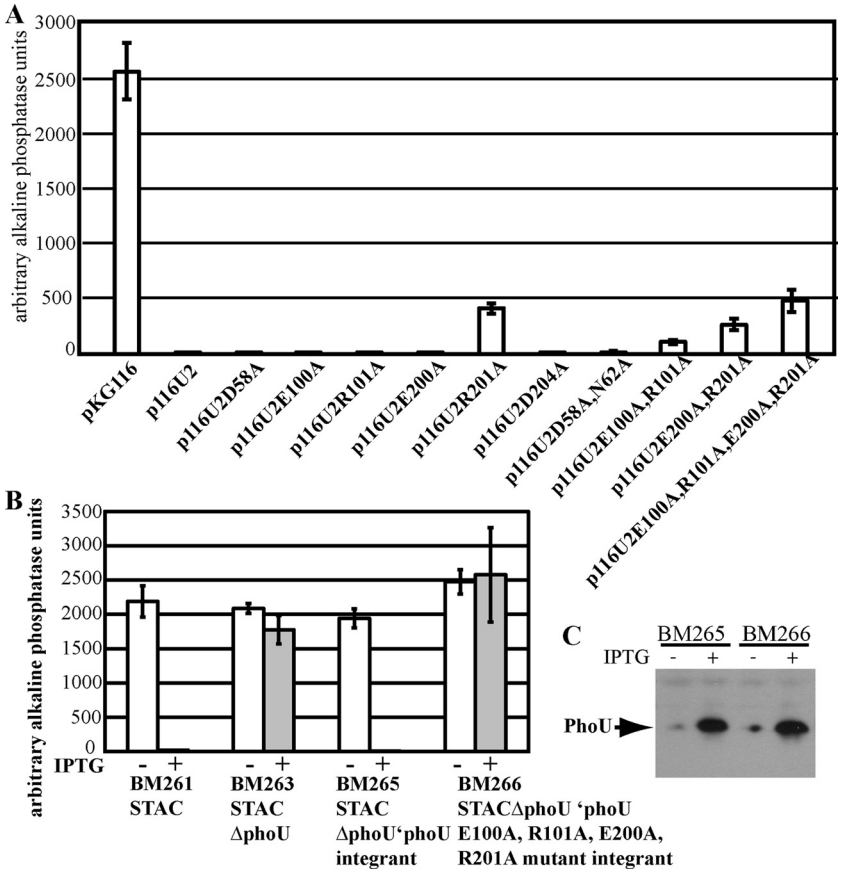

FIG 6 Signaling phenotypes of PhoU mutants. (A) Alkaline phosphatase expression was used as a reporter of P_i signaling. Plasmids with the mutant *phoU* constructs were introduced into a strain for which the native P_{pst} promoter was replaced by the P_{tac} promoter. For ease in referring to this strain, it is called STAC, for *Pst*S operon, P_{tac} promoter. A Δ*phoU* STAC strain (BM263) was used to test *phoU* mutants for signaling. Assays were performed in triplicate, and the error bars represent ± standard deviations of the measurements. (B) Signaling phenotypes of the integrated *phoU* constructs. Cells were grown overnight on a roller drum at 37°C in MOPS HiP_i medium in the presence or absence of 50 μM IPTG, and AP assays were performed in triplicate. The error bars represent ± standard deviations. (C) BM265 (*phoU*) and BM266 (*phoU*Quad) were grown in the presence or absence of 50 μM IPTG in MOPS HiP_i and then harvested and processed for visualizing protein expression by immunoblot analysis.

helix bundle to alter residues predicted to bind metal (E100A and E200A) as well as mutations of two other highly conserved residues (R101A and R201A). This version of PhoU also retained ~80% of its signaling activity.

Analysis of *phoU* integrants. Since the mutations were carried on a medium-copy-number plasmid, we postulated that the lack of a prominent phenotype was due to elevated expression levels rather than to those residues not being important for function. To address this possibility, we engineered two new strains, BM265 and BM266, which inserted the wild-type *phoU* gene or the *phoU*Quad variant into the chromosome of the Δ*phoU* strain BM263 at its normal location. AP assays were performed with strains that were grown overnight in MOPS HiP_i medium with or without 50 μM IPTG. This amount of IPTG was found to be the minimal amount needed to achieve full repression of the Pho regulon in BM261 (a strain for which the native P_{pst} promoter was replaced by the P_{tac} promoter). Analysis of the parent strain BM261 showed that repression of the Pho regulon required expression of the *pstSCAB-phoU* operon as AP was derepressed in the absence of IPTG (Fig. 6B). The Pho regulon was induced both in the presence and absence of IPTG in the Δ*phoU* strain BM263. The strain containing the integrated *phoU* gene showed a response that was indistinguishable from that of the BM261 parent strain, indicating that the reconstruction of the *pstSCAB-phoU* operon was functional and was regulated in a normal pattern. However, the *phoU*Quad mutant showed a pattern that was like that of the Δ*phoU* strain BM263, indicating that when expressed at lower levels from the chromosome, the PhoUQuad mutant was not functional. We performed Western blotting to ensure that the signaling differences between the $phoU^+$ construct and the *phoU*Quad mutant were not due to differences in protein expression or protein stability (Fig. 6C). These results support the conclusion that elevated expression of *phoU* from a multicopy-number plasmid suppresses the phenotype of the site-directed *phoU* mutations.

We hypothesized that these conserved sites may be involved in targeting PhoU to its proper cellular location. When it is expressed from a plasmid, there may be sufficient PhoU throughout the cell so that targeted membrane localization is not required for signal transmission. However, proper cellular targeting would be essential for signaling when the *phoU* gene is present in single copy and expression levels are low. To test this membrane affinity hypothesis for these conserved residues, plasmids expressing several *phoU* mutants were introduced into the Δ*phoU* strain BM263, and membrane localization experiments were performed. The amount of PhoU in the membrane fraction progressively de-

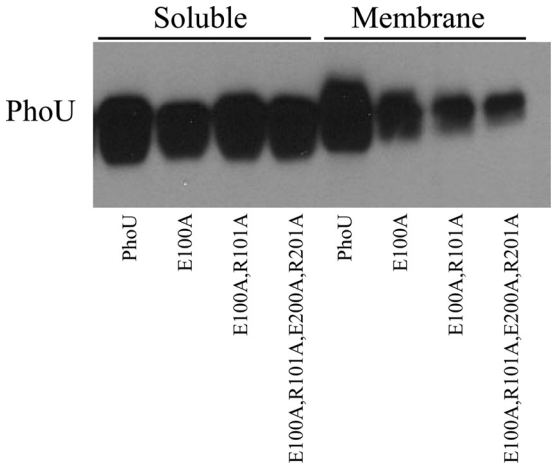

FIG 7 Membrane localization of PhoU and its mutant derivatives. BM263 cells harboring p116U2 or several derived plasmids carrying mutations that alter conserved residues were grown at 37°C in LB medium. Cells were disrupted, and the cell components were separated into soluble and membrane fractions by ultracentrifugation. A total of 1.5 μg of proteins from the soluble fractions and 5 μg from the membrane fractions were separated by SDS-PAGE, transferred to nitrocellulose, and probed with polyclonal rabbit antiserum to PhoU.

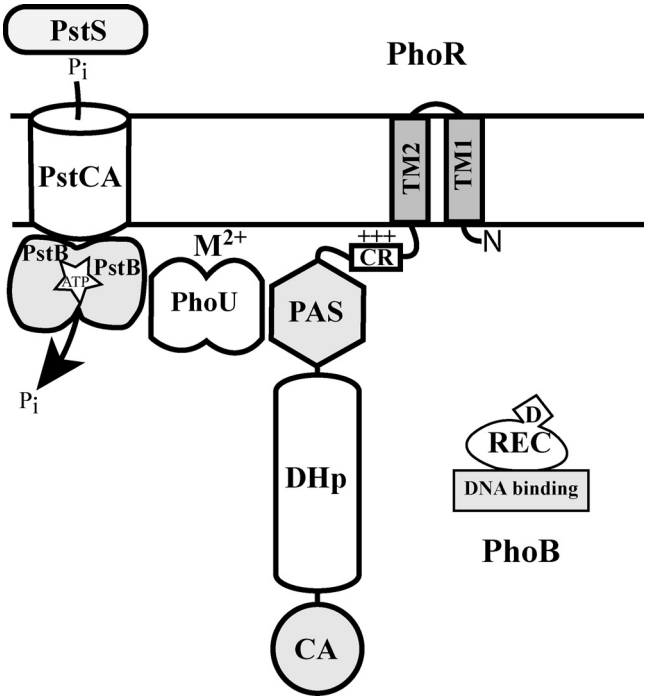

FIG 8 Model of Pho regulon expression control. PhoR contains two transmembrane segments (TM1 and TM2), a charged region (CR), and PAS, DHp, and CA domains. PhoR either phosphorylates or dephosphorylates the response regulator PhoB on a conserved aspartic acid residue (D) of its receiver domain (REC). Upon phosphorylation, PhoB binds DNA and activates expression of Pho regulon genes. The PstSCAB transporter may signal P_i levels through the alternating conformations that are inherent to its transport process. Thus, PhoU may respond to mechanical forces in its interaction with the PstSCAB transporter and transmit that information to PhoR through its PAS domain. Proper signaling complex formation requires PhoU to localize to the cytoplasmic face of the inner membrane. Metal binding (M^{2+}) by PhoU is important for its interaction with the membrane, especially when expressed at low levels, as is the case when cells are grown under phosphate-replete conditions.

creased as the number of mutations in PhoU increased from zero to four (Fig. 7).

Biochemical analysis of the PhoUQuad protein. We analyzed the PhoUQuad mutant protein for dimer formation and metal binding. When examined by gel filtration chromatography, the PhoUQuad protein eluted from the column at the same volume as the PhoU-His protein (see Fig. S1 in the supplemental material). Moreover, the PhoUQuad mutant interacted with itself in the BACTH assay (Fig. 4D). Gel filtration experiments analyzing PhoU-His with buffers that contained either EDTA to chelate metal or excess manganese to saturate metal binding did not produce any changes in the elution profiles (see Fig. S2). From these observations, we conclude that PhoU forms a dimer and that the E100, R101, E200, and R201 residues are not essential for dimer formation.

We also tested the purified PhoU-His Quad F194W protein using the fluorescence assay to measure metal binding and found that it did not bind manganese as well as PhoU-His F194W (K_d of 85.2 μM ± 26.3 versus a K_d of 18.3 μM ± 6.2 with no overlap of 94% confidence intervals of the calculated K_ds based on triplicate tests). The fluorescence peak shift observed with PhoU-His Quad F194W was significantly less than the shift caused by PhoU-His F194W (4.2 nm for the F194W mutant versus 1.7 nm for the "Quad" F194W mutant; *P* value of 0.020 from a two-tailed *t* test). We did not observe fluorescence enhancement when the PhoUQuadF194W protein was reacted with magnesium. Since the wild-type and mutant proteins both form dimers and the mutant protein does not appear to bind metals as well, we conclude that PhoU dimerization is independent of metal binding. In addition, mutations in predicted metal binding residues did not disrupt interactions with PhoR when they were assayed using the BACTH system.

DISCUSSION

This work provides evidence that the PhoU, PhoR, and PstB proteins physically interact. The demonstration of this interaction is important because it provides a framework for understanding P_i signal transduction. Our current model of this signaling pathway is that PhoU is required for the formation of a signaling complex that is comprised of PstSCAB and PhoR (Fig. 8). We propose that PhoU contains multiple nonoverlapping binding sites where it interacts with the membrane, PhoR, and PstB.

We found that PhoU's interaction with PhoR requires the PAS domain of PhoR (Fig. 2B). PAS domains often function in signaling through sensing physical or chemical stimuli (53). Structural studies of histidine kinases have shown that the correct spatial positioning of the DHp and CA domains is essential for their kinase and phosphatase activities (54–57). In some cases, it is thought that physical interactions between the CA and DHp domains lead to phosphatase activity and that altering these interactions upon receiving a signal allows for autokinase activity (57). There have also been several studies of PAS domain structures in histidine kinases (53, 56, 58, 59). In one study, the authors proposed that the PAS domain interacts with the CA domain to inhibit the CA/DHp domain interaction that is required for kinase activity and that signal binding to the PAS domain frees up the CA domain and allows for kinase activity (59). Disruption of the interactions between the PAS domain and other domains may lead

to changes in activity (55). One example reported that the PAS domain is essential for kinase function (60), while another found that the PAS domain is essential for phosphatase function (61). Clearly, PAS domains play a role in regulating the activity of many histidine kinases. Our data support a model in which the PAS domain of PhoR receives its input through direct interactions with PhoU. PAS domains frequently bind small molecules; our data do not address whether the PAS domain of PhoR binds a small molecule that allows it to interact with PhoU.

According to our signaling complex model, PhoR is able to sense through PhoU the conformational states of PstSCAB as a consequence of P_i transport and then modulate its kinase/phosphatase equilibrium toward the appropriate response. This model could accommodate variations in which the signaling complex is stable regardless of the activity of the Pst transporter or the possibility that the complex is transient and is formed only under a subset of conditions. For example, under high-P_i conditions, PstB may interact with PhoU and favor the binding of PhoR at the PAS domain. This may allow the PAS domain to interact with the CA domain and shift the activity toward phospho-PhoB phosphatase activity. Conversely, under low-P_i conditions, PhoU may not have a stable interaction with the PAS domain of PhoR, which stabilizes the autokinase activity. This hypothesis is consistent with the observed unregulated kinase activity of PhoR in the absence of PhoU or a functional PstSCAB transporter (22).

In support of a signaling complex involving PhoU, we have previously shown that PhoU modulates P_i transport through the Pst transporter (23). It seems likely that such modulation would involve direct protein interactions between PhoU and PstSCAB. Moreover, Oganesyan et al. reported that PhoU contains folds similar to Bag domains (a class of cofactors of the eukaryotic chaperone Hsp70 family) and proposed that PhoU may associate with the ATPase domain of PhoR (CA domain) and cause it to release PhoB, thus turning off the signaling cascade in a manner similar to Bag domains' association with Hsp70 (27). While supporting an interaction between PhoU and PhoR, our results show that unlike the Bag/Hsp70 paradigm, PhoU interacts with the PAS domain of PhoR and not its ATP-binding CA domain. The dimeric nature of PhoU may also be important as it interacts with the dimeric PstB and PhoR proteins.

Our data suggest that the roles of the most highly conserved residues within the PhoU protein family are to bind metal ions, which function to target PhoU to the membrane. Membrane targeting may be especially important when PhoU is present at low concentrations, such as when P_i is abundant. There are several examples where metal binding by proteins allows them to localize to the membrane. For example, annexins play a crucial role in Ca^{2+} signaling by binding Ca^{2+} that forms a bridge between the protein and the phospholipid head groups (62). Metal is bound by the protein through interactions with carbonyl and carboxyl groups of the protein and bound to the membrane through interaction with the phosphoryl moieties of the phospholipids (63). A similar mechanism is employed by the alpha-toxin protein from *Clostridium perfringens*, where binding of Ca^{2+} is linked to membrane binding and triggers the opening of the active site (64).

The highly conserved metal-binding residues of PhoU are important for signaling only when the *phoU* gene is expressed in single copy from the chromosome. They are not essential for signaling when expressed from a plasmid. It therefore seems unlikely that these residues are part of an enzymatic active site that produces a soluble message that is part of the signaling process.

By assaying for coelution of PhoU following the retention of PstB-His on a HisTrap nickel column, we were able to detect protein-protein interactions between these two proteins. We assume that this method was effective because the PstB-His protein was incorporated into a complete transporter consisting of PstC and PstA, where the proper protein conformations required for physical interactions were maintained. Coomassie stain-treated gels of the elution fractions showed many bands (not shown), including those of the predicted sizes for PstC and PstB, indicating that the affinity chromatography step enriched for the PstB-His protein but did not produce a purified complex. It seems likely that the complexity of the eluate was due to the nature of the sample applied to the column, which consisted of soluble proteins as well as proteins imbedded in membrane vesicles.

A few studies have investigated PhoU's interaction with other proteins. One group used fluorescence resonance energy transfer (FRET) analysis to determine protein-protein interactions of various proteins involved in the P_i starvation response and failed to find an interaction between PhoU and either PhoR or PhoB (65). Another study used a yeast two-hybrid assay to show that in *Edwardsiella tarda* PhoU interacts with PhoB and Fur, but they did not see any interaction with PhoR (66). However, the conflicting results between these studies imply that more evidence is necessary to fully understand all of the proteins that interact with PhoU. It is possible that fusing PhoU to enhanced cyan fluorescent protein in the FRET analysis and using a truncated PhoR protein expressed in yeast cells prevented the PhoU/PhoR interaction or the detection methods were not sensitive enough to identify the PhoU/PhoR interaction.

We used a BACTH system to identify and characterize PhoU/PhoR interactions. Others have had success using these systems to identify domains from bacterial proteins that interact and have found the BACTH system is especially useful for testing membrane bound proteins (39, 67). Our results confirm that PhoU does interact with PhoR. Given the multiple PhoR and PhoU constructs that show interaction (Fig. 2), it is unlikely that all of the different constructs are false positives. These results are also confirmed with PhoU coeluting with PhoR-His (Fig. 3).

ACKNOWLEDGMENTS

We thank John Bell, Jen Nelson, and Liz Gibbons for their assistance with the fluorescence assays and Lance Moses for help with ICP-MS analysis. We thank several undergraduate students, Geoffrey Johnston, Rachel Winn, Austin Callison, and Annaliese Gabrielle, for help in the initial characterization of the mutant strains and Casey Callison, Kirk Richardson, Michael Barrus, and Gregory Bowden for excellent technical assistance.

This work was supported by Public Health Service grant R15GM96222 from the National Institute of General Medical Sciences. R.T. was partially supported by an Undergraduate Mentoring Environment Grant from Brigham Young University.

REFERENCES

1. **Hsieh YJ, Wanner BL.** 2010. Global regulation by the seven-component P_i signaling system. Curr. Opin. Microbiol. **13:**198–203. http://dx.doi.org/10.1016/j.mib.2010.01.014.
2. **Wanner BL.** 1996. Phosphorous assimilation and control of the phosphate regulon, p 1357–1381. *In* Neidhardt FC, Curtiss R, III, Ingraham JL, Lin ECC, Low KB, Magasanik B, Reznikoff WS, Riley M, Schaechter M,

Umbarger HE (ed), *Escherichia coli* and *Salmonella*: cellular and molecular biology, 2nd ed. ASM Press, Washington, DC.
3. **Rao NN, Torriani A.** 1990. Molecular aspects of phosphate transport in *Escherichia coli*. Mol. Microbiol. **4:**1083–1090. http://dx.doi.org/10.1111/j.1365-2958.1990.tb00682.x.
4. **Torriani-Gorini A.** 1987. The birth of the Pho regulon, p 3–11. *In* Torriani-Gorini A, Rothman FG, Silver S, Wright A, Yagil E (ed), Phosphate metabolism and cellular regulation in microorganisms. American Society for Microbiology, Washington, DC.
5. **Wanner BL.** 1993. Gene regulation by phosphate in enteric bacteria. J. Cell. Biochem. **51:**47–54. http://dx.doi.org/10.1002/jcb.240510110.
6. **Makino K, Shinagawa H, Amemura M, Kawamoto T, Yamada M, Nakata A.** 1989. Signal transduction in the phosphate regulon of *Escherichia coli* involves phosphotransfer between PhoR and PhoB proteins. J. Mol. Biol. **210:**551–559. http://dx.doi.org/10.1016/0022-2836(89)90131-9.
7. **Bachhawat P, Swapna GV, Montelione GT, Stock AM.** 2005. Mechanism of activation for transcription factor PhoB suggested by different modes of dimerization in the inactive and active states. Structure (Camb.) **13:**1353–1363. http://dx.doi.org/10.1016/j.str.2005.06.006.
8. **Makino K, Amemura M, Kim S, Nakata A, Shinagawa H.** 1993. Role of the σ^{70} subunit of RNA polymerase in transcriptional activation by activator protein PhoB in *Escherichia coli*. Genes Dev. **7:**149–160. http://dx.doi.org/10.1101/gad.7.1.149.
9. **Makino K, Shinagawa H, Amemura M, Nakata A.** 1986. Nucleotide sequence of the *phoB* gene, the positive regulatory gene for the phosphate regulon of *Escherichia coli* K-12. J. Mol. Biol. **190:**37–44. http://dx.doi.org/10.1016/0022-2836(86)90073-2.
10. **McCleary WR.** 1996. The activation of PhoB by acetylphosphate. Mol. Microbiol. **20:**1155–1163. http://dx.doi.org/10.1111/j.1365-2958.1996.tb02636.x.
11. **Carmany DO, Hollingsworth K, McCleary WR.** 2003. Genetic and biochemical studies of phosphatase activity of PhoR. J. Bacteriol. **185:**1112–1115. http://dx.doi.org/10.1128/JB.185.3.1112-1115.2003.
12. **Makino K, Shinagawa H, Amemura M, Nakata A.** 1986. Nucleotide sequence of the *phoR* gene, a regulatory gene for the phosphate regulon of *Escherichia coli*. J. Mol. Biol. **192:**549–556. http://dx.doi.org/10.1016/0022-2836(86)90275-5.
13. **Etzkorn M, Kneuper H, Dunnwald P, Vijayan V, Kramer J, Griesinger C, Becker S, Unden G, Baldus M.** 2008. Plasticity of the PAS domain and a potential role for signal transduction in the histidine kinase DcuS. Nat. Struct. Mol. Biol. **15:**1031–1039. http://dx.doi.org/10.1038/nsmb.1493.
14. **Dutta R, Qin L, Inouye M.** 1999. Histidine kinases: diversity of domain organization. Mol. Microbiol. **34:**633–640. http://dx.doi.org/10.1046/j.1365-2958.1999.01646.x.
15. **Rao NN, Roberts MF, Torriani A, Yashphe J.** 1993. Effect of *glpT* and *glpD* mutations on expression of the *phoA* gene in *Escherichia coli*. J. Bacteriol. **175:**74–79.
16. **Shulman RG, Brown TR, Ugurbil K, Ogawa S, Cohen SM, den Hollander JA.** 1979. Cellular applications of ^{31}P and ^{13}C nuclear magnetic resonance. Science **205:**160–166. http://dx.doi.org/10.1126/science.36664.
17. **Peterson CN, Mandel MJ, Silhavy TJ.** 2005. *Escherichia coli* starvation diets: essential nutrients weigh in distinctly. J. Bacteriol. **187:**7549–7553. http://dx.doi.org/10.1128/JB.187.22.7549-7553.2005.
18. **Amemura M, Makino K, Shinagawa H, Kobayashi A, Nakata A.** 1985. Nucleotide sequence of the genes involved in phosphate transport and regulation of the phosphate regulon in *E. coli*. J. Mol. Biol. **184:**241–250. http://dx.doi.org/10.1016/0022-2836(85)90377-8.
19. **Rees DC, Johnson E, Lewinson O.** 2009. ABC transporters: the power to change. Nat. Rev. Mol. Cell Biol. **10:**218–227. http://dx.doi.org/10.1038/nrm2646.
20. **Webb DC, Rosenberg H, Cox GB.** 1992. Mutational analysis of the *Escherichia coli* phosphate-specific transport system, a member of the traffic ATPase (or ABC) family of membrane transporters. J. Biol. Chem. **267:**24661–24668.
21. **Davidson AL, Dassa E, Orelle C, Chen J.** 2008. Structure, function, and evolution of bacterial ATP-binding cassette systems. Microbiol. Mol. Biol. Rev. **72:**317–364. http://dx.doi.org/10.1128/MMBR.00031-07.
22. **Steed PM, Wanner BL.** 1993. Use of the *rep* technique for allele replacement to construct mutants with deletions of the *pstSCAB-phoU* operon: evidence of a new role for the PhoU protein in the phosphate regulon. J. Bacteriol. **175:**6797–6809.
23. **Rice CD, Pollard JE, Lewis ZT, McCleary WR.** 2009. Employment of a promoter-swapping technique shows that PhoU modulates the activity of the PstSCAB$_2$ ABC transporter in *Escherichia coli*. Appl. Environ. Microbiol. **75:**573–582. http://dx.doi.org/10.1128/AEM.01046-08.
24. **Surin BP, Dixon NE, Rosenberg H.** 1986. Purification of the PhoU protein, a negative regulator of the pho regulon of *Escherichia coli* K-12. J. Bacteriol. **168:**631–635.
25. **Liu J, Lou Y, Yokota H, Adams PD, Kim R, Kim SH.** 2005. Crystal structure of a PhoU protein homologue: a new class of metalloprotein containing multinuclear iron clusters. J. Biol. Chem. **280:**15960–15966. http://dx.doi.org/10.1074/jbc.M414117200.
26. **Madej T, Addess KJ, Fong JH, Geer LY, Geer RC, Lanczycki CJ, Liu C, Lu S, Marchler-Bauer A, Panchenko AR, Chen J, Thiessen PA, Wang Y, Zhang D, Bryant SH.** 2012. MMDB: 3D structures and macromolecular interactions. Nucleic Acids Res. **40:**D461–D464. http://dx.doi.org/10.1093/nar/gkr1162.
27. **Oganesyan V, Oganesyan N, Adams PD, Jancarik J, Yokota HA, Kim R, Kim SH.** 2005. Crystal structure of the "PhoU-like" phosphate uptake regulator from *Aquifex aeolicus*. J. Bacteriol. **187:**4238–4244. http://dx.doi.org/10.1128/JB.187.12.4238-4244.2005.
28. **Hoffer SM, Tommassen J.** 2001. The phosphate-binding protein of *Escherichia coli* is not essential for P$_i$-regulated expression of the *pho* regulon. J. Bacteriol. **183:**5768–5771. http://dx.doi.org/10.1128/JB.183.19.5768-5771.2001.
29. **Rao NN, Wang E, Yashphe J, Torriani A.** 1986. Nucleotide pool in pho regulon mutants and alkaline phosphatase synthesis in *E. coli*. J. Bacteriol. **166:**205–211.
30. **Datsenko KA, Wanner BL.** 2000. One-step inactivation of chromosomal genes in *Escherichia coli* K-12 using PCR products. Proc. Natl. Acad. Sci. U. S. A. **97:**6640–6645. http://dx.doi.org/10.1073/pnas.120163297.
31. **Miller J.** 1992. A short course in bacterial genetics: a laboratory manual and handbook for *Escherichia coli* and related bacteria. Cold Spring Harbor Laboratory Press, Cold Spring Harbor, NY.
32. **Yamada M, Makino K, Amemura M, Shinagawa H, Nakata A.** 1989. Regulation of the phosphate regulon of *Escherichia coli*: analysis of mutant *phoB* and *phoR* genes causing different phenotypes. J. Bacteriol. **171:**5601–5606.
33. **Buron-Barral MC, Gosink KK, Parkinson JS.** 2006. Loss- and gain-of-function mutations in the F1-HAMP region of the *Escherichia coli* aerotaxis transducer Aer. J. Bacteriol. **188:**3477–3486. http://dx.doi.org/10.1128/JB.188.10.3477-3486.2006.
34. **Studdert CA, Parkinson JS.** 2005. Insights into the organization and dynamics of bacterial chemoreceptor clusters through in vivo crosslinking studies. Proc. Natl. Acad. Sci. U. S. A. **102:**15623–15628. http://dx.doi.org/10.1073/pnas.0506040102.
35. **Blomfield IC, Vaughn V, Rest RF, Eisenstein BI.** 1991. Allelic exchange in *Escherichia coli* using the *Bacillus subtilis sacB* gene and a temperature-sensitive pSC101 replicon. Mol. Microbiol. **5:**1447–1457. http://dx.doi.org/10.1111/j.1365-2958.1991.tb00791.x.
36. **Sambrook J, Fritsch RF, Maniatis T.** 1989. Molecular cloning: a laboratory manual, 2nd ed. Cold Spring Harbor Laboratory Press, Cold Spring Harbor, NY.
37. **Neidhardt FC, Bloch PL, Smith DF.** 1974. Culture medium for enterobacteria. J. Bacteriol. **119:**736–747.
38. **Kelley LA, Sternberg MJ.** 2009. Protein structure prediction on the Web: a case study using the Phyre server. Nat. Protoc. **4:**363–371. http://dx.doi.org/10.1038/nprot.2009.2.
39. **Battesti A, Bouveret E.** 2012. The bacterial two-hybrid system based on adenylate cyclase reconstitution in *Escherichia coli*. Methods **58:**325–334. http://dx.doi.org/10.1016/j.ymeth.2012.07.018.
40. **Griffith KL, Wolf RE, Jr.** 2002. Measuring beta-galactosidase activity in bacteria: cell growth, permeabilization, and enzyme assays in 96-well arrays. Biochem. Biophys. Res. Commun. **290:**397–402. http://dx.doi.org/10.1006/bbrc.2001.6152.
41. **Thibodeau SA, Fang R, Joung JK.** 2004. High-throughput beta-galactosidase assay for bacterial cell-based reporter systems. Biotechniques **36:**410–415.
42. **Zundel CJ, Capener DC, McCleary WR.** 1998. Analysis of the conserved acidic residues in the regulatory domain of PhoB. FEBS Lett. **441:**242–246. http://dx.doi.org/10.1016/S0014-5793(98)01556-7.
43. **Ruiz N, Silhavy TJ.** 2003. Constitutive activation of the *Escherichia coli* Pho regulon upregulates *rpoS* translation in an Hfq-dependent fashion. J. Bacteriol. **185:**5984–5992. http://dx.doi.org/10.1128/JB.185.20.5984-5992.2003.
44. **Schurdell MS, Woodbury GM, McCleary WR.** 2007. Genetic evidence

suggests that the intergenic region between *pstA* and *pstB* plays a role in the regulation of *rpoS* translation during phosphate limitation. J. Bacteriol. **189:**1150–1153. http://dx.doi.org/10.1128/JB.01482-06.

45. **Baba T, Ara T, Hasegawa M, Takai Y, Okumura Y, Baba M, Datsenko KA, Tomita M, Wanner BL, Mori H.** 2006. Construction of *Escherichia coli* K-12 in-frame, single-gene knockout mutants: the Keio collection. Mol. Syst. Biol. **2:**1–11. http://dx.doi.org/10.1038/msb4100050.
46. **Vivian JT, Callis PR.** 2001. Mechanisms of tryptophan fluorescence shifts in proteins. Biophys. J. **80:**2093–2109. http://dx.doi.org/10.1016/S0006-3495(01)76183-8.
47. **Anjem A, Varghese S, Imlay JA.** 2009. Manganese import is a key element of the OxyR response to hydrogen peroxide in *Escherichia coli*. Mol. Microbiol. **72:**844–858. http://dx.doi.org/10.1111/j.1365-2958.2009.06699.x.
48. **Waters LS, Sandoval M, Storz G.** 2011. The Escherichia coli MntR miniregulon includes genes encoding a small protein and an efflux pump required for manganese homeostasis. J. Bacteriol. **193:**5887–5897. http://dx.doi.org/10.1128/JB.05872-11.
49. **Golynskiy MV, Gunderson WA, Hendrich MP, Cohen SM.** 2006. Metal binding studies and EPR spectroscopy of the manganese transport regulator MntR. Biochemistry **45:**15359–15372. http://dx.doi.org/10.1021/bi0607406.
50. **Silver S, Johnseine P, King K.** 1970. Manganese active transport in *Escherichia coli*. J. Bacteriol. **104:**1299–1306.
51. **Alatossava T, Jutte H, Kuhn A, Kellenberger E.** 1985. Manipulation of intracellular magnesium content in polymyxin B nonapeptide-sensitized Escherichia coli by ionophore A23187. J. Bacteriol. **162:**413–419.
52. **Lopez C, Sanchez J, Hermida L, Zulueta A, Marquez G.** 2004. Cysteine mediated multimerization of a recombinant dengue E fragment fused to the P64k protein following immobilized metal ion affinity chromatography. Protein Expr. Purif. **34:**176–182. http://dx.doi.org/10.1016/j.pep.2003.11.018.
53. **Moglich A, Ayers RA, Moffat K.** 2009. Structure and signaling mechanism of Per-ARNT-Sim domains. Structure **17:**1282–1294. http://dx.doi.org/10.1016/j.str.2009.08.011.
54. **Sousa EH, Tuckerman JR, Gondim AC, Gonzalez G, Gilles-Gonzalez MA.** 2013. Signal transduction and phosphoryl transfer by a FixL hybrid kinase with low oxygen affinity: importance of the vicinal PAS domain and receiver aspartate. Biochemistry **52:**456–565. http://dx.doi.org/10.1021/bi300991r.
55. **Wang C, Sang J, Wang J, Su M, Downey JS, Wu Q, Wang S, Cai Y, Xu X, Wu J, Senadheera DB, Cvitkovitch DG, Chen L, Goodman SD, Han A.** 2013. Mechanistic insights revealed by the crystal structure of a histidine kinase with signal transducer and sensor domains. PLoS Biol. **11:**e1001493. http://dx.doi.org/10.1371/journal.pbio.1001493.
56. **Winnen B, Anderson E, Cole JL, King GF, Rowland SL.** 2013. Role of the PAS sensor domains in the *Bacillus subtilis* sporulation kinase KinA. J. Bacteriol. **195:**2349–2358. http://dx.doi.org/10.1128/JB.00096-13.
57. **Gao R, Stock AM.** 2009. Biological insights from structures of two-component proteins. Annu. Rev. Microbiol. **63:**133–154. http://dx.doi.org/10.1146/annurev.micro.091208.073214.
58. **Szurmant H, White RA, Hoch JA.** 2007. Sensor complexes regulating two-component signal transduction. Curr. Opin. Struct. Biol. **17:**706–715. http://dx.doi.org/10.1016/j.sbi.2007.08.019.
59. **Yamada S, Sugimoto H, Kobayashi M, Ohno A, Nakamura H, Shiro Y.** 2009. Structure of PAS-linked histidine kinase and the response regulator complex. Structure **17:**1333–1344. http://dx.doi.org/10.1016/j.str.2009.07.016.
60. **Echenique JR, Trombe MC.** 2001. Competence modulation by the NADH oxidase of *Streptococcus pneumoniae* involves signal transduction. J. Bacteriol. **183:**768–772. http://dx.doi.org/10.1128/JB.183.2.768-772.2001.
61. **Gutu AD, Wayne KJ, Sham LT, Winkler ME.** 2010. Kinetic characterization of the $WalRK_{Spn}$ (VicRK) two-component system of *Streptococcus pneumoniae*: dependence of $WalK_{Spn}$ (VicK) phosphatase activity on its PAS domain. J. Bacteriol. **192:**2346–2358. http://dx.doi.org/10.1128/JB.01690-09.
62. **Gerke V, Creutz CE, Moss SE.** 2005. Annexins: linking Ca^{2+} signalling to membrane dynamics. Nat. Rev. Mol. Cell Biol. **6:**449–461. http://dx.doi.org/10.1038/nrm1661.
63. **Swairjo MA, Concha NO, Kaetzel MA, Dedman JR, Seaton BA.** 1995. Ca(2+)-bridging mechanism and phospholipid head group recognition in the membrane-binding protein annexin V. Nat. Struct. Biol. **2:**968–974. http://dx.doi.org/10.1038/nsb1195-968.
64. **Titball RW, Naylor CE, Miller J, Moss DS, Basak AK.** 2000. Opening of the active site of *Clostridium perfringens* alpha-toxin may be triggered by membrane binding. Int. J. Med. Microbiol. **290:**357–361. http://dx.doi.org/10.1016/S1438-4221(00)80040-5.
65. **Baek JH, Kang YJ, Lee SY.** 2007. Transcript and protein level analyses of the interactions among PhoB, PhoR, PhoU and CreC in response to phosphate starvation in *Escherichia coli*. FEMS Microbiol. Lett. **277:**254–259. http://dx.doi.org/10.1111/j.1574-6968.2007.00965.x.
66. **Chakraborty S, Sivaraman J, Leung KY, Mok YK.** 2011. Two-component PhoB-PhoR regulatory system and ferric uptake regulator sense phosphate and iron to control virulence genes in type III and VI secretion systems of *Edwardsiella tarda*. J. Biol. Chem. **286:**39417–39430. http://dx.doi.org/10.1074/jbc.M111.295188.
67. **Mikkelsen H, Hui K, Barraud N, Filloux A.** 2013. The pathogenicity island encoded PvrSR/RcsCB regulatory network controls biofilm formation and dispersal in *Pseudomonas aeruginosa* PA14. Mol. Microbiol. **89:**450–463. http://dx.doi.org/10.1111/mmi.12287.